

# **Mapping of Mesoscale and Submesoscale Wind Fields Using Synthetic Aperture Radar**

Donald R. Thompson  
Johns Hopkins University/APL  
Johns Hopkins Road  
Laurel, MD 20723

phone: (240) 228-4559    fax: (240) 228-5548    e-mail: [donald\\_thompson@jhuapl.edu](mailto:donald_thompson@jhuapl.edu)

Robert C. Beal  
Johns Hopkins University/APL  
Johns Hopkins Road  
Laurel, MD 20723

phone: (240) 228-5009    fax: (240) 228-5548    e-mail: [robert\\_beal@jhuapl.edu](mailto:robert_beal@jhuapl.edu)

Award # N00014-96-1-0376  
<http://fermi.jhuapl.edu/stormwatch>

## **LONG-TERM GOAL**

The long-term goal of this research effort is to investigate the possibility of obtaining quantitative information about the near-surface wind field and perhaps other parameters that characterize the Marine Atmospheric Boundary Layer (MABL) from an analysis of Synthetic Aperture Radar (SAR) imagery. Because of its potential for yielding such information at high horizontal resolution, this application of SAR would represent a significant advance over most scatterometer and passive microwave sensors that yield only coarse-resolution estimates of the wind field.

## **SCIENTIFIC OBJECTIVES**

The major scientific objective of our research is to determine, by comparisons with more standard measurements and model predictions, if it is possible to extract detailed quantitative estimates of the near-surface wind field and perhaps various other parameters that characterize the MABL from SAR imagery. Because of the large footprint associated with conventional multiple-antenna scatterometers or passive microwave sensors, wind estimates in coastal regions are difficult to obtain. SAR, on the other hand, provides high-resolution imagery where various signatures associated with fluctuations in the MABL are commonly seen, especially in coastal waters. Moreover, because SAR can resolve the surface signatures of turbulence structures in the MABL, it may be possible to diagnose the surface layer stability and therefore even produce wind-speed estimates corrected for this important effect.

## **APPROACH**

Since most of the RADARSAT imagery analyzed to date has been collected in the wide ScanSar beam mode that is as yet uncalibrated, we have devised a “bootstrap” calibration procedure based on the use of NDBC buoys distributed across a subset of the imagery, that depends critically on an H-pol scatterometer algorithm we have been developing. We convert the resulting cross section image to wind speed using this algorithm along with wind-direction estimates over the spatial extent of the image

| Report Documentation Page  |                                    |                                     |   | Form Approved<br>OMB No. 0704-0188                  |                                 |
|--|------------------------------------|-------------------------------------|---|---|---------------------------------|
| Public reporting burden for the collection of information is estimated to average 1 hour per response, including the time for reviewing instructions, searching existing data sources, gathering and maintaining the data needed, and completing and reviewing the collection of information. Send comments regarding this burden estimate or any other aspect of this collection of information, including suggestions for reducing this burden, to Washington Headquarters Services, Directorate for Information Operations and Reports, 1215 Jefferson Davis Highway, Suite 1204, Arlington VA 22202-4302. Respondents should be aware that notwithstanding any other provision of law, no person shall be subject to a penalty for failing to comply with a collection of information if it does not display a currently valid OMB control number. |                                    |                                     |   |   |                                 |
| 1. REPORT DATE<br><b>1998</b>  |                                    | 2. REPORT TYPE                      |   | 3. DATES COVERED<br><b>00-00-1998 to 00-00-1998</b> |                                 |
| 4. TITLE AND SUBTITLE<br><b>Mapping of Mesoscale and Submesoscale Wind Fields Using Synthetic Aperture Radar</b>   |                                    |                                     |   | 5a. CONTRACT NUMBER                                 |                                 |
|  |                                    |                                     |   | 5b. GRANT NUMBER                                    |                                 |
|  |                                    |                                     |   | 5c. PROGRAM ELEMENT NUMBER                          |                                 |
| 6. AUTHOR(S)   |                                    |                                     |   | 5d. PROJECT NUMBER                                  |                                 |
|  |                                    |                                     |   | 5e. TASK NUMBER                                     |                                 |
|  |                                    |                                     |   | 5f. WORK UNIT NUMBER                                |                                 |
| 7. PERFORMING ORGANIZATION NAME(S) AND ADDRESS(ES)<br><b>Johns Hopkins University, Applied Physics Laboratory, 11100 Johns Hopkins Rd, Laurel, MD, 20723</b>   |                                    |                                     |   | 8. PERFORMING ORGANIZATION REPORT NUMBER            |                                 |
| 9. SPONSORING/MONITORING AGENCY NAME(S) AND ADDRESS(ES)  |                                    |                                     |   | 10. SPONSOR/MONITOR'S ACRONYM(S)                    |                                 |
|  |                                    |                                     |   | 11. SPONSOR/MONITOR'S REPORT NUMBER(S)              |                                 |
| 12. DISTRIBUTION/AVAILABILITY STATEMENT<br><b>Approved for public release; distribution unlimited</b>  |                                    |                                     |   |   |                                 |
| 13. SUPPLEMENTARY NOTES<br><b>See also ADM002252.</b>  |                                    |                                     |   |   |                                 |
| 14. ABSTRACT   |                                    |                                     |   |   |                                 |
| 15. SUBJECT TERMS  |                                    |                                     |   |   |                                 |
| 16. SECURITY CLASSIFICATION OF:  |                                    |                                     | 17. LIMITATION OF ABSTRACT<br><b>Same as Report (SAR)</b> | 18. NUMBER OF PAGES<br><b>5</b>                     | 19a. NAME OF RESPONSIBLE PERSON |
| a. REPORT<br><b>unclassified</b>   | b. ABSTRACT<br><b>unclassified</b> | c. THIS PAGE<br><b>unclassified</b> |   |   |                                 |

obtained from now-casts supplied to us daily by FNMOC. The resulting high-resolution wind-field maps are then compared with other lower-resolution sensors as well as NDBC buoys.

## TASKS COMPLETED

- During the months of October to March 1997-1998 and 1998-1999, we have been (and will be) acquiring wide-ScanSar mode RADARSAT images covering the coastal ocean along the entire east coast of North America as part of the NOAA StormWatch Program. A detailed map of this coverage and the corresponding dates for 1998-99 may be viewed on the StormWatch web site at: <http://fermi.jhuapl.edu/sar/stormwatch/> click "RADARSAT Coverage".
- Development of a suitable H-pol scatterometer algorithm, begun during last year's effort, is continuing. Although the RADARSAT ScanSar beam modes are still uncalibrated, we have made use of (fully-calibrated) standard-beam images with concurrent *in situ* wind field measurements from aircraft and buoys to validate and tune our H-pol algorithms.
- Since the wide-ScanSar imagery is not yet calibrated by RADARSAT, we are presently using scenes in which several NDBC buoys are distributed across the image swath to develop a "boot-strap" calibration by forcing the radar cross section at the buoy location to be such that our H-pol scatterometer algorithm yields the buoy wind speed. This calibration is then tested on other scenes.
- Now-casts from the FNMOC model analysis to account for wind direction variability over the area of our RADARSAT scenes are now used along with the calibration techniques and H-pol scatterometer algorithm discussed above for the generation of high-resolution wind maps.
- Our wind-map generation procedure has been automated so that high-resolution wind maps can be generated from the SAR image within about 30 minutes after the image file is received.

## RESULTS

As part of the NOAA StormWatch program, we are presently receiving wide ScanSAR (450 km swath) imagery over the coastal Atlantic off the eastern US during the winter months of 1997-98 and 1998-99. This imagery is processed by the Alaska SAR Facility (ASF). Details of the StormWatch Program and the precise area of SAR coverage are described in [1, 2]. Since the backscatter cross section for microwave scattering from a wind-driven ocean surface depends on the direction of the wind vector with respect to the radar look-direction, an estimate of this direction over the extent of the SAR image is needed. Determination of the local wind direction is one of the major difficulties that must be overcome for reliable SAR wind mapping. Previous studies [3, 4] have indicated that large-scale ( $\sim$  km) structures present in the SAR imagery, especially for unstable MABL conditions, can sometimes provide an indication of the wind direction. We have however, found several cases where this technique can be quite misleading. Our present approach therefore is to incorporate predictions for the wind direction from the Fleet Numerical Meteorology and Oceanography Center (FNMOC) into our wind-mapping procedure. As discussed in [2], we receive these predictions each day at 2400 ( $\sim$  1.5 h after the SAR overpasses) and 1200 (UT) on a  $1^\circ \times 1^\circ$  grid from FNMOC.

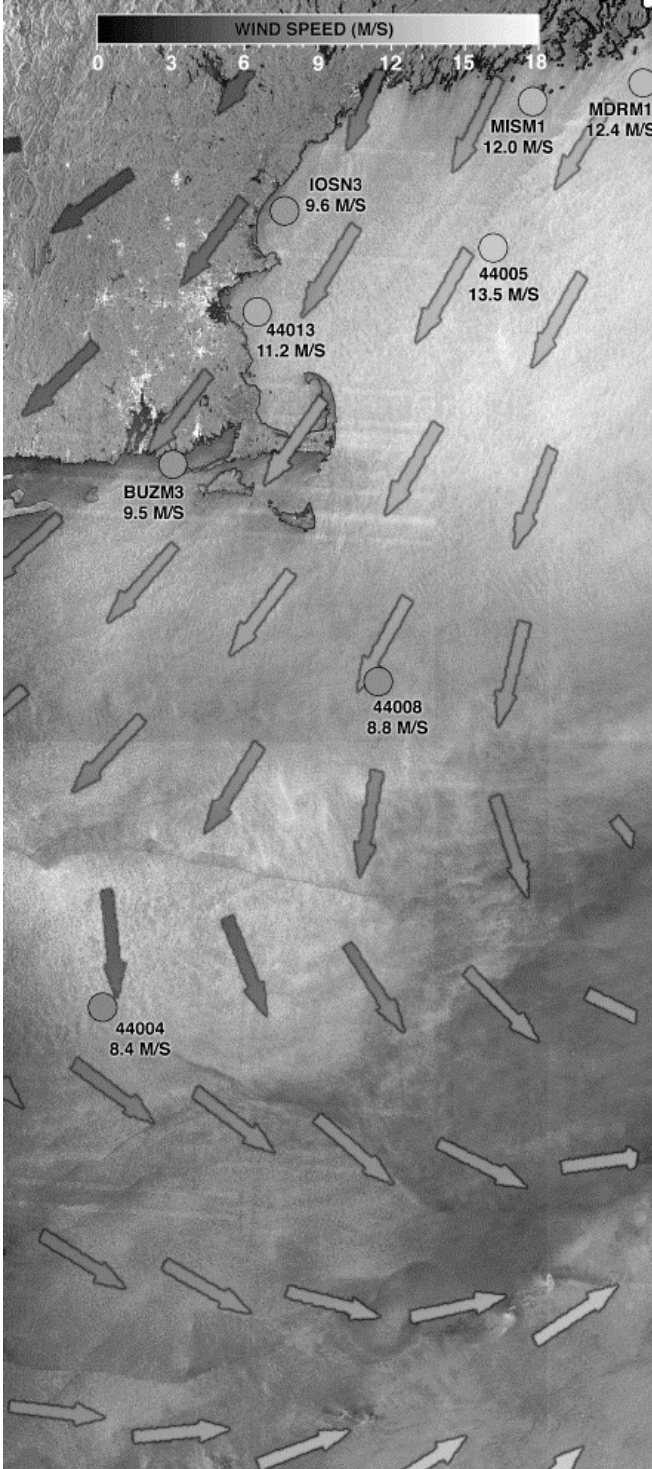


Figure 1. Wind map generated from RADARSAT orbit 10710. The arrows show the predicted FNMOC wind direction. The gray-scale of the arrows and NDBC buoys match that used for the SAR wind field, and reflects the corresponding wind-speed as measured at the buoy or predicted by the model.

In order to convert the imagery into wind maps, we need to know a relationship between the radar cross section,  $\sigma_0$ , and the local wind velocity; i.e. a scatterometer algorithm. A relatively well-tested algorithm, CMOD4, developed for the C-band V-pol, ERS-1 scatterometer already exists [5]. Since RADARSAT operates at H-pol however, CMOD4 cannot be used directly. As a preliminary technique for dealing with this problem, we have modified the V-pol CMOD4 algorithm that predicts  $\sigma_0^V(U, \theta, \phi)$  for use at H-pol using the hybrid expression

$$\sigma_0^H = \frac{(1 + \alpha \tan^2 \theta)^2}{(1 + 2 \tan^2 \theta)^2} \sigma_0^V(U, \theta, \phi), \quad (1)$$

where  $U$  is the wind speed,  $\theta$  is the incidence angle,  $\phi$  is the azimuth angle of the radar with respect to the wind direction, and  $\sigma_0^H$  is the resulting H-pol cross section. The simple (empirical) polarization ratio used in (1) yields good agreement with measured H-pol cross sections for incidence angles between about  $20^\circ$  to  $40^\circ$  [6], and reproduces curves similar to those given in the paper by Campbell and Vachon [7] when the value for the parameter  $\alpha$  is chosen to be 0.6. The Bragg scattering polarization ratio is given by (1) when  $\alpha$  is zero and when  $\alpha = 1$ ,  $\sigma_0^H$  equals the Kirchhoff cross section [8].

For specified values of  $\theta$  and  $\phi$ , and  $\sigma_0^H$ -values from the SAR image, we can now find the corresponding wind-speed values by inverting equation (1). The  $\theta$ -value at each pixel in the RADARSAT image is specified by the satellite geometry. We use the wind-direction field obtained from the FNMOC model prediction for the overpass time to interpolate the appropriate  $\phi$ -value at each pixel. Unfortunately, the RADARSAT wide ScanSar beam mode is not yet properly calibrated so we must use a “bootstrap” procedure to proceed further. What we have done is to use a ScanSar scene where there are NDBC buoys positioned across the image swath, and determine a calibration coefficient at the position of these buoys such that the resulting cross sections yield the buoy wind speed from our hybrid scatterometer algorithm. Although this procedure is somewhat circular, we

can use the calibration coefficients determined in this manner to calibrate other scenes where buoy data is not available. We expect calibrated ScanSar imagery to be available in the near future.

In Figure 1, we show a wind map generated from a RADARSAT image collected during orbit 10710 (22:30 UT on 22.11.97) at a resolution of 300 m pixels. We have converted this image to a wind map using the procedures outlined above. Shown in the northern portion of this figure are shaded circles representing 8 NDBC buoys with their measured wind vectors at the overpass time. The circles at each buoy are shown with a gray-scale level to represent the measured wind speed using the same scale as the image itself. (These gray-scale levels agree quite closely with that of the resulting wind map; as they must with our “bootstrap” calibration scheme.) The FNMOC wind directions are also shown in this way with the gray scale representing the model-predicted wind speed. Note that these speeds are independent of the calibration. One can see by the visibility of the model wind vectors against the background SAR-wind field in Figure 1 that large-scale variations in these two (independent) quantities agree quite well. The smaller-scale variations that are quite apparent in the SAR wind field are, of course, not present in the FNMOC model.

Comparison with AVHRR imagery shows that the narrow dark band evident in the middle portion of the wind map in Figure 2 marks the north wall of the Gulf Stream. In this area, the SAR wind field is characterized by regions of high wind-speed variance resulting from the turbulence produced by an unstable MABL. In the next version of our wind extraction implementation, we plan to use the FNMOC air and sea-surface temperature fields as well as AVHRR SSTs to correct the extracted wind speeds for MABL stability.

Clearly, our SAR wind-extraction procedure contains errors whose magnitude depends on the fidelity of the calibration procedure as well as knowledge of the “true” SAR wind algorithm. Furthermore, improved understanding of the importance of the various “contaminating” influences from oceanic processes unrelated to the wind field will clearly affect the accuracy of the wind maps. Nevertheless, as we improve our ability to recognize and properly account for these influences, we expect that the accuracy of the resulting SAR wind estimates will exceed anything currently possible in near-coastal regions, especially when the SAR image can be nested within other pertinent atmospheric and oceanic fields.

## **IMPACT FOR SCIENCE**

As outlined above, SAR has the potential to overcome some of the inherent limitations of conventional scatterometry. We expect our approach for mapping mesoscale and submesoscale wind fields using synthetic aperture radar will not only provide more information on a higher resolution than do existing algorithms, but will also allow diagnoses to be performed much closer to strong discontinuities such as coasts and ocean current boundaries. Furthermore, remote measurements of the small-scale structure in the wind field, i.e. the wind-speed variance, which are only possible with high-resolution SARs, can provide an indication of the atmospheric stability and possibly even quantitative estimates of the stability parameter.

## **RELATIONSHIP TO OTHER PROGRAMS**

The work described above is part of a collaboration with meteorologists at The Pennsylvania State University. Two doctoral students at Penn State, for whom we served as thesis committee members,

have been awarded their Ph.D. degree for research related to SAR wind extraction. The RADARSAT wide ScanSar imagery examined in this research was obtained as part of the NOAA Stormwatch Program.

## REFERENCES

1. Beal, R. C. and W. G. Pichel, "StormWatch 97–98 and beyond: Application of SAR as a high-resolution scatterometer in coastal regions," *1998 IEEE International Geoscience and Remote Sensing Symposium Proceedings III*, 1379-1381, 1998.
2. Monaldo, F. M., and R. C. Beal, "Toward real-time processing, blending, and dissemination of operational wind products from the RADARSAT SAR", *1998 IEEE International Geoscience and Remote Sensing Symposium Proceedings: III*, 959-961, 1998.
3. Gerling, T. W., "Structure of the surface wind field from SeaSat SAR", *J. Geophys. Res.*, **91**, 2308-2320, 1987.
4. Fetterer, F., D. Ginereis, C. C. Wackerman, "Validating a scatterometer wind algorithm for ERS-1 SAR," *IEEE Trans. Geosci. Remote Sensing*, **36**, 479–492 1997.
5. Stoffelen, A. and D. L. T. Anderson, "Wind retrieval and ERS-1 scatterometer radar backscatter measurements", *Adv. Space Res.*, **13**, 53-60, 1993.
6. Unal, C. M. H., P. Snooji, P. J. F. Swart, "The polarization-dependent relation between radar backscatter from the ocean surface and surface wind vectors at frequencies between 1 and 18 GHz", *IEEE Trans. Geosci. Remote Sensing*, **29**, 621-626, 1991.
7. Campbell, J. W. M., and P. W. Vachon, "Extracting ocean wind vectors from satellite imagery", *Backscatter*, **8** (2), 16-21, 1997.
8. Thompson, D. R., Tanos Elfouhaily, and Bertrand Chapron, "Polarization ratio for microwave backscattering from the ocean surface at low to moderate incidence angles", *1998 IEEE International Geoscience and Remote Sensing Symposium Proceedings III*, 1671-1673, 1998.